Dalton Transactions

RSC Publishing

PAPER

View Article Online
View Journal | View Issue

Cite this: *Dalton Trans.*, 2013, **42**, 9746

Novel self-assembled supramolecular architectures of Mn(II) ions with a hybrid pyrazine–bipyridine ligand†‡

Monika Wałęsa-Chorab,[a] Maciej Kubicki,[a] Maria Korabik[b] and Violetta Patroniak*[a]

Received 4th February 2013,
Accepted 24th April 2013

DOI: 10.1039/c3dt50352f

www.rsc.org/dalton

A new hybrid pyrazine–bipyridine ligand **L** ($C_{26}H_{20}N_6$) and its complexes with $Mn(NO_3)_2$, $Mn(ClO_4)_2$, $MnCl_2$ and $MnBr_2$ have been synthesised. By the self-assembly of **L** and Mn(II) ions three different kinds of supramolecular complexes have been obtained: binuclear baguette complex $[Mn_2\mathbf{L}(H_2O)_6](NO_3)_4{\cdot}2.5H_2O$ **1** and tetranuclear [2 × 2] grid-type complex $[Mn_4\mathbf{L}_4](ClO_4)_8{\cdot}2.5(CH_3CN){\cdot}2CH_3OH$ **2** and mononuclear complexes $[Mn\mathbf{L}_2]X_2$ (where $X = Cl^-$ **3** and $X = Br^-$ **4**). Crystal structures and magnetic properties of Mn(II) complexes **1** and **2** have been also investigated. The crystal structures reveal that in both **1** and **2** complexes the Mn(II) ions have coordination number 6 and distorted octahedral coordination geometry. In **2** four metal cations and four ligands have assembled into a grid-type [2 × 2] array, with a perchlorate anion occupying the central cavity, with clearly a good fit for the center of the cavity. The perchlorate anion, in contrast to the nitrate anion, probably acts as a template in the formation of tetranuclear grid-type complexes. Magnetic susceptibility measurements indicate that the Mn(II) ions are all high spin, and in both **1** and **2** complexes there are weak antiferromagnetic interactions between Mn(II) ions.

Introduction

By a spontaneous combination of organic electron-donor ligands with electron-deficient metal ions (self-assembly or self-sorting)[1,2] it is possible to obtain metallasupramolecular architectures such as two-dimensional squares, triangles, and polygons,[3] as well as three-dimensional cages[4,5] and metal–organic frameworks.[6,7]

Binuclear complexes in which metal ions' coordination sphere is filled with labile anions or solvent molecules are attractive compounds for catalysis.[8,9] Such complexes can be also building blocks for construction of multinuclear compounds.[10] Binuclear baguette complexes in which metal ions are bridged by pyridine or pyrazine rings are very attractive mainly in the field of magnetic materials.[11–14]

Grid-type complexes are architectures in which ligands and metal ions form a rectangular or square array and in which ligands that form nodes are crossed.[15] The design of grid-like complexes relies on the directing coordination algorithms, comprising the number and arrangement of donor atoms in a ligand molecule and the preferred coordination geometry of the metal ion.[16] The structure of supramolecular complexes depends strongly on the ligand substituent, the ligand conformation, the metal ion, the counterion, the solvent, and the reaction conditions. Newton *et al.*[17] reported that the N-donor ligand consisting of three pyridine groups linked by two pyrazole moieties, thus forming one tridentate and two bidentate binding sites, forms a heptanuclear bimetallic helical complex of Fe(II)–Co(II) and the nonanuclear heterometallic grid complex; conversion of the helix into a grid is possible *via* changing the Fe–Co molar ratio. The reversible conversion of the pincer-like complex into the grid-like architecture can be modulated also *via* changing the nature of the solvent.[18] Formation of grid complexes depending on the pH value has been also reported.[19,20] In most cases, grids are found as single molecules and do not have the possibility of aggregation because metal ions do not have labile ligands or vacant sites. Such aggregation is possible when ligand molecules contain donor atoms able to coordinate to more than one metal ion[21] or groups which can form hydrogen bonds.[22] It has been also shown that grids can be absorbed onto the surface (*e.g.* graphite) to give an ordered monolayer.[23,24] Grid-type supramolecular architectures have been very interesting in the last few years mainly because of the square topology of the metal ions. Such topology of metal ions can generate interesting magnetic, optical or redox properties. Grid-type complexes have potential applications such as molecular-scale sensors, switches and information storage devices in nanotechnology.[25–27] Grids play also an important role in the host–guest chemistry because they can accommodate anions[28] or small molecules[29] in their cavities.

[a]*Faculty of Chemistry, Adam Mickiewicz University, Umultowska 89b, 61614 Poznań, Poland. E-mail: violapat@amu.edu.pl*
[b]*Faculty of Chemistry, University of Wrocław, 14 Joliot-Curie, 50383 Wrocław, Poland*

†Dedicated to Professor Jacek Gawroński on his 70th birthday.

‡CCDC 883804 (**1**) and 919104 (**2**). For crystallographic data in CIF or other electronic format see DOI: 10.1039/c3dt50352f

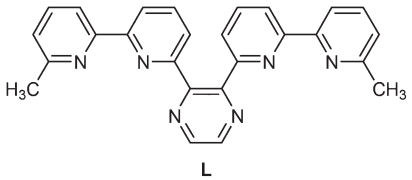

Fig. 1 The ligand **L**.

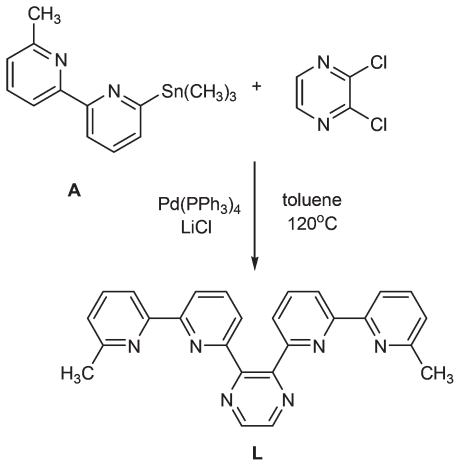

Scheme 1 Synthesis of ligand **L**.

Manganese complexes are attracting considerable interest in the field of bioinorganic chemistry as models of active sites of enzymes.[30] The Mn^{2+} ions have a high spin and slow electronic relaxation, and their complexes are attractive alternatives for Gd^{3+} complexes in the design of contrast agents for magnetic resonance imaging.[31]

Hybrid pyrazine–bipyridine ligands are already known to form mono- and binuclear rack-type complexes of Ru(II)[32,33] and binuclear complexes of Co(II) ions.[34,35]

We reported that the hybrid pyrazine–terpyridine N_8-donor ligand can act as either a quaterpyridine–terpyridine or a simple terpyridine binding unit towards transition metal ions and that it forms binuclear complexes of either M_2L or M_2L_2 stoichiometry.[36] In view of successful synthesis of grid-type complexes of Cu(I), Ag(I), Zn(II), Co(II) and Fe(II)[37–40] we have attempted to prepare new N_6-donor pyrazine-bis(bipyridine) ligand **L** 2,3-bis(6′-methyl-2,2′-bipyridin-6-yl)pyrazine (Fig. 1).

The ligand **L** which contains two terpyridine-like subunits in the process of self-assembling with Mn(II) salts forms three types of supramolecular complexes: binuclear baguette complex **1**, tetranuclear [2 × 2] grid-type complex **2** and mononuclear complexes **3**, **4**. The ligand **L** and Mn(II) complexes have been characterized by spectroscopic and analytical methods. X-ray structures and magnetic properties of **1** and **2** complexes have been also determined.

Results and discussion

Synthesis of ligand L

Related to **L**, hybrid pyrazine–bipyridine ligands have been obtained using a multistep condensation reaction.[41] We decided to obtain the ligand **L** in a simpler way, using the Stille-type coupling reaction as outlined in Scheme 1.

2-(6-Methylpyridin-2-yl)-6-(trimethylstannyl)pyridine (**A**) was prepared by the catalytic reaction of 2-bromo-6-(6-methylpyridin-2-yl)pyridine with hexamethylditin[42] and was used in the Stille-type coupling reaction with 2,3-dichloropyrazine in the presence of Pd(0) catalyst and LiCl. The ligand **L** has been obtained in 66% yield as a white powder.

Synthesis and structures of Mn(II) complexes

The supramolecular complexes have been obtained by self-assembly of ligand **L** and $Mn(NO_3)_2$, $Mn(ClO_4)_2$, $MnCl_2$ and $MnBr_2$. Reactions were carried out in a 1 : 1 metal-to-ligand molar ratio in nitromethane solution at room temperature for 48 h. Two complexes of Mn(II) ions were readily isolated by precipitation as yellow stable solids. Self-assembly of **L** and Mn(II) salts, depending on the nature of counterions, leads to formation of three types of supramolecular complexes. The dinuclear baguette complex $[Mn_2\mathbf{L}(H_2O)_6](NO_3)_4{\cdot}2.5H_2O$ **1** was obtained when nitrate anions were present in the reaction mixture. In the presence of perchlorate anions [2 × 2] grid-type complex $[Mn_4\mathbf{L}_4](ClO_4)_8$ **2** has been obtained (which contains also some water and other solvent molecules, *cf.* the Experimental part). Reactions of **L** with halogen salts (chloride and bromide) lead to formation of mononuclear complexes with a 1 : 2 metal-to-ligand stoichiometry formulated as $[Mn\mathbf{L}_2]X_2$ (where X = Cl^- **3** and X = Br^- **4**). The single crystals suitable for X-ray analysis were obtained by slow evaporation of diethyl ether (for complex **1**) or toluene (for complex **2**) into nitromethane solutions of complexes. The ESI-MS spectra of **1** displayed peaks *e.g.* at *m*/*z* = 712 and *m*/*z* = 730 unambiguously assigned to the molecular cations $[Mn_2(\mathbf{L})(NO_3)_3]^+$ and $[Mn_2(\mathbf{L})(NO_3)_3(H_2O)]^+$, which suggests that in solution there exist different species of complex **1** in which the coordination sphere of Mn(II) ions is filled by nitrate anions or nitrate anions and water molecules. The ESI-MS spectra of **3** and **4** consist of peaks at *m*/*z* = 444 corresponding to the $[Mn\mathbf{L}_2]^{2+}$ molecular cation, which indicates the formation of mononuclear complexes in which the metal ion coordinates with two ligand molecules. The formation of this type of complex has been also confirmed by elemental analysis. In the IR spectra of **2** there are two overlapped bands at about 1100 cm^{-1} from perchlorate anions, which suggests that the anion lying inside the cavity of **2** has lower symmetry than anionic perchlorate. In the crystal structure between the encapsulated perchlorate anion and the cation complex there are many short contacts (*cf.* Fig. 6), which result in weak 'pseudo-bidentate' spectroscopic behavior. The lowering of symmetry of perchlorate anions has been also observed for Cu(II) complexes with a terpyridine ligand.[43] In that case it was caused by strong hydrogen bonds in the crystal lattice.

Fig. 2 and 3 show the perspective views of the cations. In both complexes the Mn cations are 6-coordinated in the

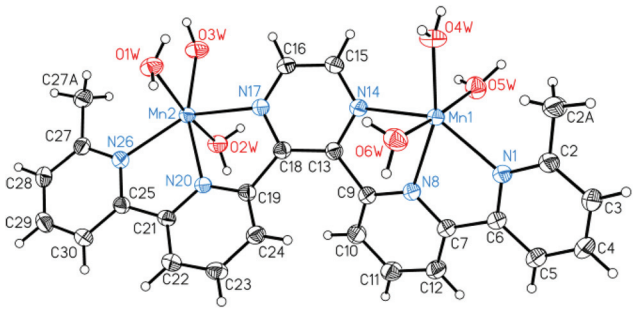

Fig. 2 Perspective view of the cation **1**; ellipsoids are drawn at 50% probability level, hydrogen atoms are shown as spheres of arbitrary radii. Relevant distances (Å): Mn1–N1 2.2499(16), Mn1–N8 2.2211(16), Mn1–N14 2.3337(16), Mn1–O4W 2.1392(14), Mn1–O5W 1.1258(15) Å, Mn1–O6W 2.1749(15), Mn2–N17 2.3209(16), Mn2–N20 2.2203(15), Mn2–N26 2.2412(16), Mn2–O1W 2.1990(15), Mn2–O2W 2.1706(14), Mn2–O3W 2.1317(14), and angles (°): N1–Mn1–N14 143.11(6), N8–Mn1–O4W 161.77(6), O5W–O6W 171.64(6)., N17–Mn2–N26 142.08(6), N20–Mn2–O3W 161.39(6), O1W–Mn2–O2W 165.80(5).

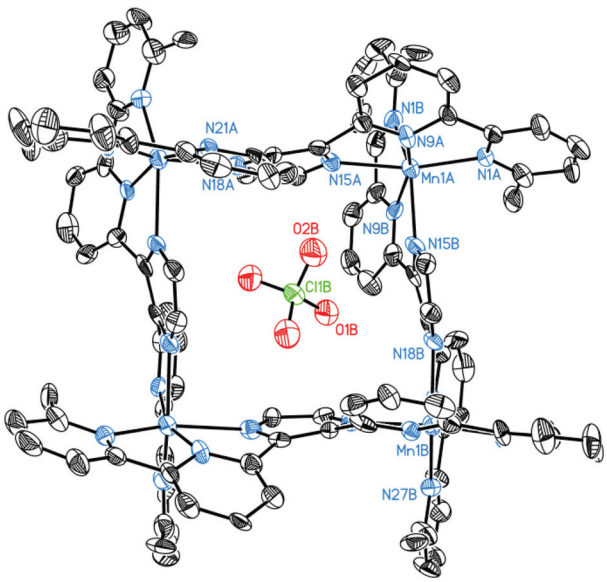

Fig. 3 Perspective view of the cation **2**; ellipsoids are drawn at 33% probability level, hydrogen atoms are omitted for clarity. One central symmetrical ClO_4^- anion is also shown. Relevant distances (Å): Mn1A–N1A 2.225(9), Mn1A–N9A 2.206(10), Mn1A–N15A 2.328(8), Mn1A–N1B 2.244(10), Mn1A–N9B 2.213(9), Mn1A–N15B 2.295(8), Mn1B–N18B 2.361(8), Mn1B–N21B 2.205(9), Mn1B–N27B 2.249(9), Mn1B–N18A′ 2.295(8), Mn1B–N21A′ 2.204(8), Mn1B–N27A′ 2.251(10), and angles (°): N1A–Mn1A–N15A 144.9(4), N9A–Mn1A–N9B 160.1(3), N1B–Mn1A–N15B 144.9(4), N18B–Mn1B–N27B 144.1(3), N21B–Mn1B–N21A′ 159.9(3), N18A′-Mn1B-N27A′ 145.8(3). Prime denotes the symmetry operation (1 – *x*, –*y*, *z*).

distorted octahedral fashion. The distortions are caused mainly by the ligand geometry, and as a result the largest L–Mn–L angles are in the range 140–160° (instead of ideal 180°).

In complex **1** one ligand coordinates to two different Mn cations, using two "bay areas"; the coordination sphere for each Mn is filled by three water molecules, which in turn are engaged in very complicated hydrogen-bond systems with the nitrate ions and solvent water molecules. In the ligand each

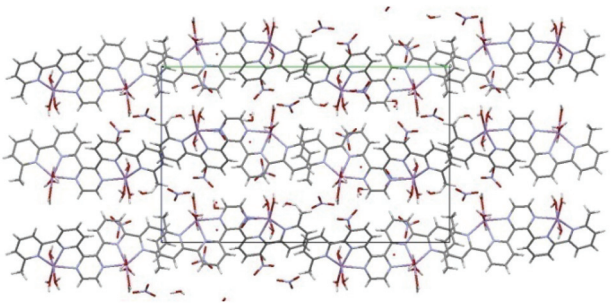

Fig. 4 The crystal packing of **1** as seen along the *a* axis.

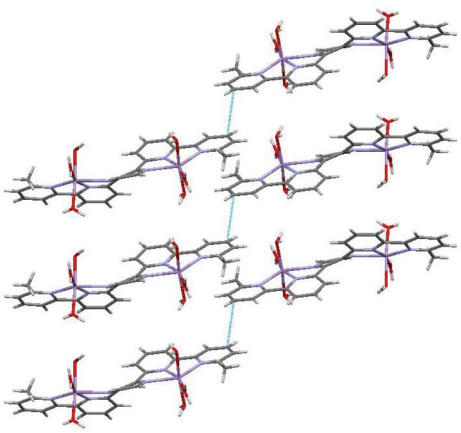

Fig. 5 The arrangement of complex cations of **1** in sheets. Short contacts are depicted as dashed, light-blue lines.

pair of terminal rings is relatively coplanar (dihedral angles between the ring planes are 5.57(5)° and 10.20(6)°, while these planes are more inclined with respect to the central pyrazine ring plane (31.71(5)° and 28.53(5)°). The dihedral angle between the terminal ring planes, which can be regarded as a measure of overall shape of the ligand, is 42.91(5)°, which is a little bit smaller than in a similar ligand – which is the only similar structure deposited in the Cambridge Crystallographic database,[44] 2,3-bis(6-(2,2′-bipyridyl))pyrazine – where it is 64.6°.[41]

In the crystal lattice of **1** the cations form sheets parallel to the *b* axis (and columns parallel to the *a* axis) separated by nitrate anions and solvent molecules (Fig. 4).

Within one sheet complex cations lying side by side have an opposite arrangement; water molecules coordinating to Mn(II) ions are directed in one way (down *c* axis) in one complex molecule and in the other way (up *c* axis) in the adjacent complex molecule (Fig. 5).

In **2** four cations and four ligand molecules form the symmetric ring (or square), lying across the crystallographic twofold axis (on which also the Cl atom of one perchlorate anion lies) in the space group *Aba*2. The four Mn(II) ions do not lie on one plane; the Mn···Mn···Mn···Mn intra-ring dihedral angle is 12.53°.

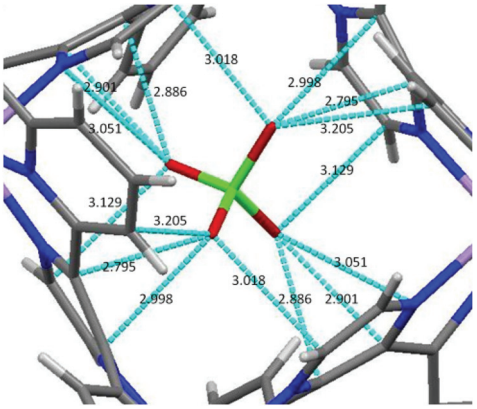

Fig. 6 Presentation of the short contacts between the encapsulated perchlorate anion and the cavity of the complex.

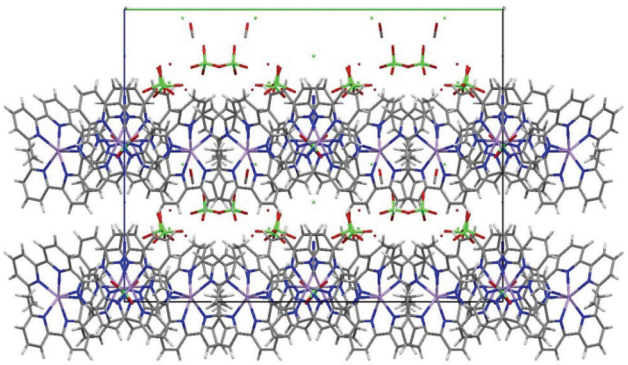

Fig. 7 The crystal packing of **2** as seen along the *a* axis.

Two symmetry-independent Mn···Mn distances are 7.339 Å and 7.351 Å; diagonal distances between manganese ions are similar, 10.041 and 10.601 Å. Inside the cavity in the coordination cation there is one C_2-symmetrical perchlorate anion. The encapsulated perchlorate anion is clearly a good fit for the center of the cavity and probably can act as a template in the formation of tetranuclear [2 × 2] grid complexes. A similar templating effect was observed for tetrafluoroborate anions in the formation of tetranuclear circular helicates.[45] Encapsulated perchlorate anions interact with the cavity by many short contacts (Fig. 6), which makes the perchlorate anion have lower symmetry than the anionic one.

The dihedral angles between the aromatic rings in two ligand fragments are generally larger than in **1** – probably in order to allow for this certain, cyclic accommodation of four such molecules – but the dihedral angles between the terminal rings are similar (22.2(7)° and 33.9(6)°). In the crystal lattice of **2** cation complexes form sheets parallel to the *b* axis (Fig. 7).

Similar sheets are seen along the *b* axis (Fig. 8a). Within adjacent sheets cation complexes do not lie one above the other but adjacent sheets are moved relative to each other.

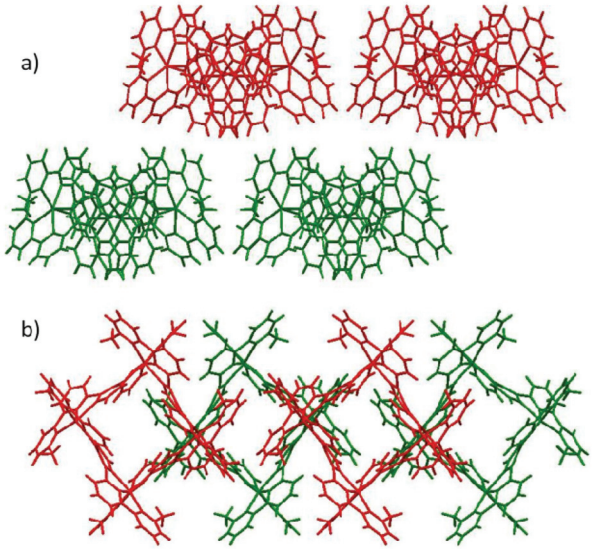

Fig. 8 The crystal packing of **2** as seen along (a) *b* axis (b) *c* axis. Anions and solvent molecules are omitted for clarity.

Magnetic properties

The magnetic properties of **1** and **2** were measured in the temperature range 1.8–300 K at 0.5 T and are presented in Fig. 9.

For both complexes, the $\chi_m T$ product *versus* the temperature has a constant value from room temperature to *ca.* 100 K, of 4.56 cm^3 K mol^{-1} for **1** and 4.36 cm^3 K mol^{-1} for **2** (magnetic susceptibility χ_m was calculated per one Mn^{II} ion), which is expected for noninteracting S = 5/2 ions. $\chi_m T$ drops slowly between 100 and *ca.* 30 K, and then sharply below 30 K to reach values of *ca.* 2.55 cm^3 K mol^{-1} for **1** and 2.02 cm^3 K mol^{-1} for **2** at 2 K. This behavior is indicative of antiferromagnetic exchange interactions between the manganese(II) ions.

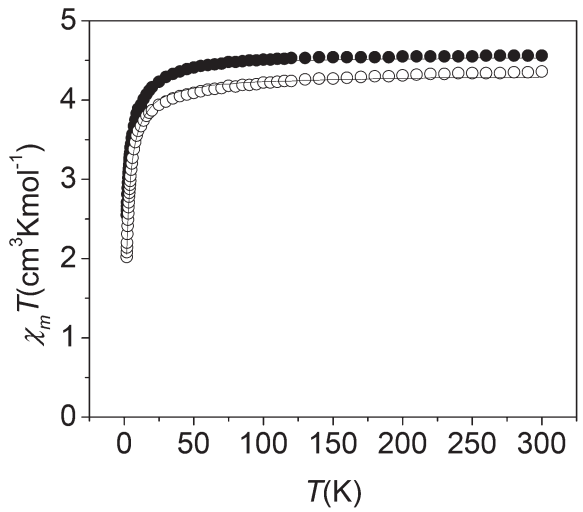

Fig. 9 The $\chi_m T$ *versus* the temperature relation for 1 (●) and 2 (○). Solid lines indicate the best fit (see the text).

The theoretical calculation of the thermally accessible energy levels of the magnetic properties of a binuclear Mn(II) complex is performed using the Hamiltonian $H = -JS_1S_2$. The appropriate formula is[46]

$$\chi = \frac{Ng^2\beta^2}{kT}\frac{e^x + 5e^{3x} + 14e^{6x} + 30e^{10x} + 55e^{15x}}{1 + 3e^x + 5e^{3x} + 7e^{6x} + 9e^{10x} + 11e^{15x}}$$

where $x = J/kT$.

The best parameters obtained with this model are as follows: $J = -0.22 \pm 0.02$ cm^{-1}; $g = 2.02 \pm 0.01$; $R = 8.4 \times 10^{-5}$.

In order to fit the magnetic susceptibility data of **2**, a simple model with only one J[47–51] and $H = -J(S_1 \cdot S_2 + S_2 \cdot S_3 + S_3 \cdot S_4)$ as spin Hamiltonian was initially assumed, with analytical expression:

$$\chi_m = [Ng\beta S(S+1)(1+u)]/[3kT(1-u)]$$

here $S = 5/2$, and u is the well-known Langevin function,[51]

$$u = \coth[JS(S+1)/kT] - kT/JS(S+1).$$

The best fit leads to $J = -0.29 \pm 0.01$ cm^{-1}, $g = 2.0 \pm 0.1$, and $R = 1.8 \times 10^{-4}$. The $\chi_m T$ *vs.* T plots for both complexes fit well to the models used, as indicated by the calculated curves (Fig. 9). Comparable exchange parameters ($J = -0.22 \pm 0.02$ cm^{-1} and $J = -0.29 \pm 0.01$ cm^{-1} for **1** and **2**, respectively) confirmed a similar in-plane pyrazine bridged mode.

Very weak antiferromagnetic interactions between high spin manganese ions in compounds **1** and **2** were confirmed by magnetization *versus* field measurements at 2 K (Fig. 10). Experimental points are below the curve of $S = 5/2$.

Weak antiferromagnetic interactions along the diazine ring have been observed in some other manganese derivatives.[52–54]

The ability of the pyrazine bridge to mediate magnetic interactions between paramagnetic centers, separated by more than 6.5 Å, has been well characterized in the literature. The largest antiferromagnetic coupling has been found in the case of copper(II) complexes ($J = -61.1$ cm^{-1},[55] $J = -40.9$ cm^{-1} [56]).

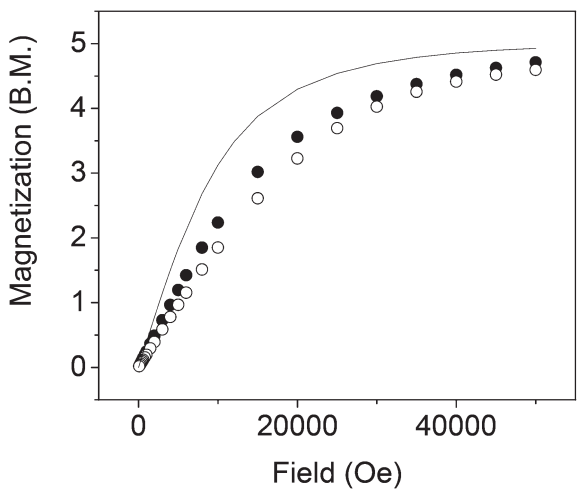

Fig. 10 Magnetization *versus* magnetic field relations for **1** (●) and **2** (○), at 2 K. Solid line is the Brillouin function for $S = 5/2$, $g = 2$.[46]

Table 1 Selected structural parameters of both complexes

	Compound **1**	Compound **2**
Mn–N_{pyz} distances (Å)		2.325(9)
	2.3337(16)	2.298(10)
	2.3209(16)	2.359(9)
		2.293(9)
Mn–N_{pyz}···N_{pyz} angles (°)	162.5	169.7; 172.0
	169.1	166.9; 172.7
Displacement of the Mn ion from the mean plane of the bridge (Å)	0.675	0.371; −0.260
	−0.413	0.477; −0.312
Mn···Mn distances (Å)	7.323	7.338; 7.350
J (cm^{-1})	−0.22	−0.29
n^2J (cm^{-1})	−5.50	−7.25

Nevertheless, most of the examples show weak antiferromagnetic interactions ($|J| < 4$ cm^{-1}).[57,58] In general the magnetic coupling is antiferromagnetic, resulting from a net overlap of magnetic orbitals through the pyrazine bridge. Dinuclear manganese(II) complexes bridged by pyrazine derivatives, studied recently,[59] show very weak antiferromagnetic coupling, with exchange parameters J of −0.16 cm^{-1}, and −0.26 cm^{-1}, comparable to those obtained for the analyzed complexes **1** and **2**. Because different numbers of magnetic orbitals in the case of high spin manganese(II) complexes are present, the value of n^2J instead of J (n being the number of magnetic orbitals) was proposed to be more appropriate for comparison of magnetic interactions.[59–61] The n^2J values of compounds **1** ($5^2J = -5.50$ cm^{-1}) and **2** ($5^2J = -7.25$ cm^{-1}) show more strong magnetic interactions in the grid-type architecture of square topology of manganese(II) ions.

In Table 1 some structural parameters, related to the bridging system, are extracted to explain small differences in magnetic coupling between **1** and **2**. A similar analysis of copper(II) complexes leads to the conclusion that displacement of the metal from the mean plane of the pyrazine bridge is the main factor which increases the antiferromagnetic coupling because it allows a σ-overlap between the metal $d_{x^2-y^2}$ magnetic orbitals and the π-orbitals of the pyrazine ring.[58] In manganese(II) complexes the magnetic interactions are more complex. Structural parameters of both **1** and **2** complexes (Table 1) are comparable. Taking into account the displacement of the Mn(II) ions from the mean plane of the bridge an opposite relation is observed. Smaller displacement existing in **2** can lead to better overlap through π-pathways, which increases the $|J_\pi|$ component of magnetic interactions and finally higher magnetic coupling is observed in **2** than in **1**.

Experimental

General consideration

The metal salts were used without further purification as supplied from Aldrich. NMR spectra were run on a Varian Gemini 300 MHz spectrometer and were calibrated against the residual protonated solvent signals ($CDCl_3$ δ 7.24) and shifts are given in ppm. ESI mass spectra for acetonitrile solutions ~10^{-4} M were measured using a Waters Micromass ZQ spectrometer.

FAB mass spectra were run on a Bruker 320MS/450GC spectrometer. Melting point was obtained using the EZ-MELT MPA120 apparatus. Melting point was measured in the range of temperatures 30–400 °C, ramp rate 2 °C min^{-1}. Microanalyses were obtained using a Vario EL III CHN element analyzer. IR spectra were obtained with a Bruker FT-IR IFS 66/s spectrometer and peak positions are reported in cm^{-1}. Magnetization measurements in the temperature range of 1.8–300 K were carried out on powdered samples of complexes, at the magnetic field 0.5 T, using a Quantum Design SQUID Magnetometer (type MPMS-XL5). A polycrystalline sample for magnetic measurements was obtained from single crystals. Corrections for diamagnetism of the constituting atoms were calculated using Pascal's constants.[46] The effective magnetic moments were calculated from the expression:

$$\mu_{\text{eff}} = 2.83\sqrt{\chi_{\text{m}}^{\text{corr}} \cdot T}\,(\text{B.M.})$$

The best exchange parameters were obtained by fitting with a good agreement factor R defined as follows:

$$R = \sum_{i=1}^{n} \frac{(\chi_i^{\text{exp}}T - \chi_i^{\text{calc}}T)^2}{(\chi_i^{\text{exp}}T)^2}$$

Standard deviations[62] were added to calculated exchange parameters.

Synthesis of 2,3-bis(6′-methyl-2,2′-bipyridin-6-yl)pyrazine L. To a mixture of crude 2-(6-methylpyridin-2-yl)-6-(trimethylstannyl)pyridine (**A**) (1.805 g, 5.4 mmol), 2,3-dichloropyrazine (0.321 g, 2.2 mmol), $Pd(PPh_3)_4$ (0.320 g, 0.3 mmol) and LiCl (1.012 g, 23.5 mmol), 100 ml of degassed toluene was added gradually *via* a syringe, constantly maintaining an argon atmosphere. The reaction mixture was stirred under reflux for 24 hours at 120 °C and subsequently the solvent was removed under reduced pressure on a rotary evaporator. Purification by means of chromatography on alumina with CH_2Cl_2–*n*-hexane (1 : 1 v : v) as an eluent yielded 0.591 g (66%) of white powder. Mp: 170.0–172.1 °C. FAB-MS: *m*/*z* (%) = 417.3 (M^+, 100). IR (KBr): ν = ν(C–H)$_{ar}$ 3068, 3057, 3042; $\nu_{as}(CH_3)$ 2963; $\nu_s(CH_3)$ 2923; ν(C=C) 1594, 1571, 1529, 1470; ν(C=N) 1439, 1400, 1382, 1371, 1263; ρ(C–H) 1148, 1114, 1083, 1048; γ(C–H) 993, 902, 856, 830, 788, 742, 633 cm^{-1}. ^{1}H NMR ($CDCl_3$, 300 MHz): δ = 8.65 (s, 2H), 8.29 (d, 2H, J = 7.6 Hz), 7.97 (d, 2H, J = 7.6 Hz), 7.95 (t, 2H, J = 7.7 Hz), 7.30 (t, 2H, J = 7.8 Hz), 7.14 (d, 2H, J = 7.8 Hz), 6.95 (d, 2H, J = 7.6 Hz), 2.48 (s, 6H, CH_3) ppm. Elemental analysis calcd for $C_{26}H_{20}N_6$ (416.48): C, 74.98; H, 4.84; N, 20.18. Found: C, 74.96; H, 4.82; N, 20.20%.

$[Mn_2(\mathbf{L})(H_2O)_6](NO_3)_4{\cdot}2.5H_2O$ **1**: A mixture of ligand **L** (23.1 mg, 55 μmol) and $Mn(NO_3)_2{\cdot}4H_2O$ salt (13.8 mg, 55 μmol) in nitromethane (20 mL) was stirred at room temperature for 48 h under the normal atmosphere. The complex **1** was isolated as a yellow solid by evaporation of the solvent and recrystallisation of the residue from the minimum volume of CH_3CN by the gradual addition of ethyl ether. Yield: 73%. ESI-MS: *m*/*z* (%) = 730 (10) $[Mn_2(\mathbf{L})(NO_3)_3(H_2O)]^+$, 712 (10) $[Mn_2(\mathbf{L})(NO_3)_3]^+$, 533 (50) $[Mn(\mathbf{L})(NO_3)]^+$, 417 (10) $[\mathbf{L} + H]^+$, 262 (10) $[Mn(\mathbf{L})(H_2O)_3]^{2+}$, 236 (20) $[Mn(\mathbf{L})]^{2+}$, 159 (30) $[Mn_2(\mathbf{L})(H_2O)_6]^{4+}$. IR (KBr): ν = ν(C–H)$_{ar}$ 3080; $\nu_{as}(CH_3)$ 2954; $\nu_s(CH_3)$ 2925; ν(C=C) 1607, 1597, 1573, 1466; ν(C=N) 1432, 1247; $\nu(NO_3^-)$ 1384, 1309, 792; ρ(C–H) 1182, 1114, 1093, 1071, 1049; γ(C–H) 830, 741, 719, 660, 634 cm^{-1}. Elemental analysis calcd for $[Mn_2(C_{26}H_{20}N_6)(H_2O)_6](NO_3)_4{\cdot}2.5H_2O$ (927.50): C, 33.67; H, 4.02; N, 15.10. Found: C, 33.68; H, 4.03; N, 15.08%.

$[Mn_4(\mathbf{L})_4](ClO_4)_8{\cdot}2.5(CH_3CN){\cdot}2CH_3OH$ **2**: A mixture of ligand **L** (25.4 mg, 60 μmol) and $Mn(ClO_4)_2{\cdot}6H_2O$ salt (21.7 mg, 60 μmol) in nitromethane (20 mL) was stirred at room temperature for 48 h under the normal atmosphere. The complex **2** was isolated as a yellow solid by evaporation of the solvent and recrystallisation of the residue from the minimum volume of CH_3CN by the gradual addition of ethyl ether. Yield: 64%. ESI-MS: *m*/*z* (%) = 570 (20) $[Mn(\mathbf{L})(ClO_4)]^+$, 444 (20) $[Mn(\mathbf{L})_2]^{2+}$, 417 (10) $[\mathbf{L} + H]^+$, 236 (70) $[Mn(\mathbf{L})]^{2+}$. IR (KBr): ν = ν(C–H)$_{ar}$ 3090; $\nu_s(CH_3)$ 2925; ν(C=C) 1608, 1598, 1573, 1479, 1466; ν(C=N) 1452, 1436, 1414, 1383, 1337, 1310, 1253; ρ(C–H) 1185, 1172, 1036, 1017; $\delta(ClO_4^-)$ 1096, 1093; γ(C–H) 833, 825, 795, 746, 724, 699, 675, 664, 644 $\nu(ClO_4^-)$ 624 cm^{-1}. Elemental analysis calcd for $[Mn_4(C_{26}H_{20}N_6)_4](ClO_4)_8{\cdot}2.5(CH_3CN){\cdot}2CH_3OH$ (2848.00): C, 46.81; H, 3.38; N, 13.03; Found: C, 46.79; H, 3.40; N, 13.02%.

$[Mn(\mathbf{L})_2]Cl_2$ **3**: A mixture of ligand **L** (16.0 mg, 38 μmol) and $MnCl_2{\cdot}4H_2O$ salt (7.5 mg, 38 μmol) in nitromethane (20 mL) was stirred at room temperature for 48 h under the normal atmosphere. The complex **3** was isolated as a yellow solid by evaporation of the solvent and recrystallisation of the residue from the minimum volume of CH_3CN by the gradual addition of ethyl ether. Yield: 58%. ESI-MS: *m*/*z* (%) = 506 (30) $[Mn(\mathbf{L})Cl]^+$, 444 (10) $[Mn(\mathbf{L})_2]^{2+}$, 439 (50) $[Na(\mathbf{L})]^+$, 417 (10) $[\mathbf{L} + H]^+$, 236 (20) $[Mn(\mathbf{L})]^{2+}$. IR (KBr): ν = ν(C–H)$_{ar}$ 3055; $\nu_{as}(CH_3)$ 2961; $\nu_s(CH_3)$ 2920; ν(C=C) 1590, 1568; ν(C=N) 1417, 1397, 1384, 1261; ρ(C–H) 1166, 1096, 1037; γ(C–H) 875, 802, 713, 598, 527 cm^{-1}. Elemental analysis $[Mn(C_{26}H_{20}N_6)_2]Cl_2$ (958.80) calcd: C, 65.14; H, 4.21; N, 17.53. Found: C, 65.15; H, 4.20; N, 17.52%.

$[Mn(\mathbf{L})_2]Br_2$ **4**: A mixture of ligand **L** (20.7 mg, 50 μmol) and $MnBr_2{\cdot}4H_2O$ salt (14.3 mg, 50 μmol) in nitromethane (20 mL) was stirred at room temperature for 48 h under the normal atmosphere. The complex **4** was isolated as a yellow solid by evaporation of the solvent and recrystallisation of the residue from the minimum volume of CH_3CN by the gradual addition of ethyl ether. Yield: 66%. ESI-MS: *m*/*z* (%) = 551 (10) $[Mn(\mathbf{L})Br]^+$, 444 (10) $[Mn(\mathbf{L})_2]^{2+}$, 236 (25) $[Mn(\mathbf{L})]^{2+}$. IR (KBr): ν = ν(C–H)$_{ar}$ 3064, 3052; $\nu_s(CH_3)$ 2918; ν(C=C) 1604, 1596, 1572, 1477, 1464; ν(C=N) 1432, 1413, 1384, 1307, 1250; ρ(C–H) 1184, 1170, 1113, 1092, 1070, 1016; γ(C–H) 836, 799, 745, 720, 697, 663, 634, 558 cm^{-1}. Elemental analysis $[Mn(C_{26}H_{20}N_6)_2]Br_2$ (1047.70) calcd: C, 59.61; H, 3.85; N, 16.04. Found: C, 59.64; H, 3.80; N, 16.02%.

Single crystal structure determination

X-ray diffraction data were collected at room temperature by the ω-scan technique on Agilent Technologies four-circle

Table 2 Crystal data and structural refinement parameters for Mn(II) complexes

Compound	**1**	**2**
CCDC deposition number	883804	919104
Formula	$C_{26}H_{32}Mn_2N_6O_6^{4+}\cdot 4NO_3^-\cdot 2.5(H_2O)$	$C_{104}H_{80}Mn_4N_{24}^{8+}\cdot 8ClO_4^-\cdot 2.5(CH_3CN)\cdot 2CH_3OH$
Formula weight	927.54	2848.00
Crystal system	Monoclinic	Orthorhombic
Space group	$P2_1/n$	$Aba2$
a (Å)	7.5044(4)	18.5171(7)
b (Å)	28.6866(9)	30.0858(11)
c (Å)	17.8381(8)	23.2151(10)
β (°)	101.152(5)	90
V (Å^3)	3767.6(3)	12933.2(9)
Z	4	4
d_x (g cm^{-3})	1.64	1.45
F (000)	1908	5772
μ (mm^{-1})	6.32	0.63
Θ Range (°)	2.96–73.52	2.81–25.00
hkl Range	$-9 \le h \le 9$	$-22 \le h \le 22$
	$-34 \le k \le 35$	$-35 \le k \le 35$
	$-21 \le l \le 21$	$-27 \le l \le 27$
Reflections:		
Collected	41 738	68 161
Unique (R_{int})	7530 (0.045)	11 139 (0.099)
With $I > 2\sigma(I)$	6730	6844
Weighting scheme:		
A	0.0521	0.2
B	1.1788	0
R(F) [$I > 2\sigma(I)$]	0.033	0.113
w$R(F^2)$ [$I > 2\sigma(I)$]	0.088	0.279
$R(F)$ [all data]	0.038	0.168
w$R(F^2)$ [all data]	0.092	0.312
Goodness of fit	1.04	1.06
Max/min $\Delta\rho$ (e Å^{-3})	0.33/−0.53	1.76/−0.52

diffractometers: for **1** at 130(1) K on a SuperNova (Atlas detector) with mirror-monochromatized CuK_α radiation (λ = 1.54178 Å), and for **2** at 100(1) K on an Xcalibur (Eos detector) with graphite-monochromatized MoK_α radiation (λ = 0.71073 Å). The data were corrected for Lorentz-polarization and absorption effects.[63] Accurate unit-cell parameters were determined by a least-squares fit of 21 058 (**1**), and 9331 (**2**) reflections of highest intensity, chosen from the whole experiment. The structures were solved with SIR92[64] and refined with the full-matrix least-squares procedure on F^2 by SHELXL97.[65] Scattering factors incorporated in SHELXL97 were used. All non-hydrogen atoms were refined anisotropically, all hydrogen atoms were placed in the calculated positions, and refined as a 'riding model' with the isotropic displacement parameters set at 1.2 (1.5 for methyl groups) times the U_{eq} value for appropriate non-hydrogen atoms. Hydrogen atoms from the majority of water molecules in **1** were located in the difference Fourier maps and then treated also as riding on their parent oxygen atoms. In both structures the disorder has been observed despite the low temperature data collections; in **1** it is relatively easy to model (one water molecule) while in **2** almost all anion and solvent fragments were regarded as disordered. For one apparently heavily disordered perchlorate anion we were unable to find the positions of oxygen atoms. Relevant crystal data are listed in Table 2, together with refinement details.

Conclusions

The new hybrid pyrazine–bipyridine ligand **L** was synthesized using Stille-type coupling reactions. The results reported here provide an example of inorganic self-organization of well-defined supramolecular architectures. The manganese(II) salts serve as a template to orient molecules of the ligand in the desired conformation for formation of appropriate kind of complexes. Magnetic susceptibility measurements indicate that the Mn(II) ions are all high spin, and adjacent Mn(II) ions are weakly antiferromagnetically coupled *via* a pyrazine ring in both complexes. Many compounds as multifunctional materials are made from manganese ions.[66,67]

Acknowledgements

Financial support received from the Polish National Science Centre (Grant No. 2011/01/N/ST5/02235 and NN204 198240) is gratefully acknowledged.

Notes and references

1 M. M. Safont-Sempere, G. Fernández and F. Würthner, *Chem. Rev.*, 2011, **111**, 5784.

2 K. Mahata and M. Schmittel, *J. Am. Chem. Soc.*, 2009, **131**, 16544.
3 L. Ma, B. O. Patrick and D. Dolphin, *Chem. Commun.*, 2011, **47**, 704.
4 A. Stephenson and M. D. Ward, *Dalton Trans.*, 2011, **40**, 10360.
5 C. R. K. Glasson, G. V. Meehan, C. A. Motti, J. K. Clegg, P. Turner, P. Jensen and L. F. Lindoy, *Dalton Trans.*, 2011, **40**, 10481.
6 E. C. Constable, C. E. Housecroft, M. Neuburger, S. Vujovic, J. A. Zampese and G. Zhang, *CrystEngComm*, 2012, **14**, 3554.
7 A. S. Degtyarenko, P. V. Solntsev, H. Krautscheid, E. B. Rusanov, A. N. Chernega and K. V. Domasevitch, *New J. Chem.*, 2008, **32**, 1910.
8 Q. Khamker, Y. D. M. Champouret, K. Singh and G. A. Solan, *Dalton Trans.*, 2009, 8935.
9 H.-L. Kwong, H.-L. Yeung, W.-S. Lee and W.-T. Wong, *Chem. Commun.*, 2006, 4841.
10 M. Stollenz, H. Gehring, V. Konstanzer, S. Fischer, D. Dechert, Ch. Grosse and F. Meyer, *Organometallics*, 2011, **30**, 3708.
11 T. Ishida, T. Kawakami, S. Mitsubori, T. Nogami, K. Yamaguchi and H. Iwamura, *J. Chem. Soc., Dalton Trans.*, 2002, 3177.
12 N. Chanda, B. Sarkar, J. Fiedler, W. Kaim and G. K. Lahiri, *Dalton Trans.*, 2003, 3550.
13 D. M. D'Alessandro and F. R. Keene, *New J. Chem.*, 2006, **30**, 228.
14 R. Watanebe, T. Shimada, N. Koyama, T. Ishida and T. Kogane, *Polyhedron*, 2011, **30**, 3165.
15 A. M. Stadler, *Eur. J. Inorg. Chem.*, 2009, 4751.
16 M. Ruben, J. Rojo, F. J. Romero-Salguero, L. H. Uppadine and J.-M. Lehn, *Angew. Chem., Int. Ed.*, 2004, **43**, 3644.
17 G. N. Newton, T. Onuki, T. Shiga, M. Noguchi, T. Matsumoto, J. S. Mathieson, M. Nihei, M. Nakano, L. Cronin and H. Oshio, *Angew. Chem., Int. Ed.*, 2011, **50**, 4844.
18 J. Ramírez, A.-M. Stadler, N. Kyritsakas and J.-M. Lehn, *Chem. Commun.*, 2007, 237.
19 J. Klingele, J. F. Boas, J. R. Pilbrow, B. Moubaraki, K. S. Murray, K. J. Berry, K. A. Hunter, G. B. Jameson, P. D. W. Boyd and S. Brooker, *Dalton Trans.*, 2007, 633.
20 J. Klingele, A. I. Prikhod'ko, G. Leibeling, S. Demeshko, S. Dechert and F. Meyer, *Dalton Trans.*, 2007, 2003.
21 Y. S. Moroz, S. Demeshko, M. Haukka, A. Mokhir, U. Mitra, M. Stocker, P. Müller, F. Meyer and I. O. Fritsky, *Inorg. Chem.*, 2012, **51**, 7445.
22 E. Breuning, U. Ziener, J.-M. Lehn, E. Wegelius and K. Rissanen, *Eur. J. Inorg. Chem.*, 2001, 1515.
23 A. Mourran, U. Ziener, M. Möller, E. Breuning, M. Ohkita and J.-M. Lehn, *Eur. J. Inorg. Chem.*, 2005, 2641.
24 M. Ruben, J.-M. Lehn and P. Müller, *Chem. Soc. Rev.*, 2006, 1056.
25 M. D. Allendorf, A. Schwartzberg, V. Stavila and A. A. Talin, *Chem.–Eur. J.*, 2011, **17**, 11372.
26 A. R. Stefankiewicz and J.-M. Lehn, *Chem.–Eur. J.*, 2009, **15**, 2500.
27 E. M. Zueva, E. R. Ryabikh and S. A. Borshch, *Inorg. Chem.*, 2011, **50**, 11143.
28 M. I. Ortiz, M. L. Soriano, M. P. Carranza, F. A. Jalón, J. W. Steed, K. Mereiter, A. M. Rodríguez, D. Quiñonero, P. M. Deyà and B. R. Manzano, *Inorg. Chem.*, 2010, **49**, 8828.
29 M. C. Carrión, I. M. Ortiz, F. A. Jalón and B. R. Manzano, *Cryst. Growth Des.*, 2011, **11**, 1766.
30 O. Iranzo, *Bioorg. Chem.*, 2011, **39**, 73.
31 B. Drahoš, I. Lukeš and E. Tóth, *Eur. J. Inorg. Chem.*, 2012, 1975.
32 F. Heirtzler, P. Jones, M. Neuburger and M. Zehnder, *Polyhedron*, 1999, **18**, 601.
33 F. R. Heirtzler, M. Neuburger, M. Zehnder, S. J. Bird, K. G. Orrell and V. Sik, *J. Chem. Soc., Dalton Trans.*, 1999, 565.
34 F. Heirtzler, S. Santi, K. Howland and T. Weyhermüller, *Dalton Trans.*, 2006, 4722.
35 F. Heirtzler and T. Weyhermüller, *J. Chem. Soc., Dalton Trans.*, 1997, 3653.
36 A. R. Stefankiewicz, M. Wałęsa-Chorab, J. Harrowfield, M. Kubicki, Z. Hnatejko, M. Korabik and V. Patroniak, *Dalton Trans.*, 2013, **42**, 1743.
37 V. Patroniak, A. R. Stefankiewicz, J.-M. Lehn and M. Kubicki, *Eur. J. Inorg. Chem.*, 2005, 4168.
38 V. Patroniak, P. N. W. Baxter, J.-M. Lehn, M. Kubicki, M. Nissinen and K. Rissanen, *Eur. J. Inorg. Chem.*, 2003, 4001.
39 V. Patroniak, J.-M. Lehn, M. Kubicki, A. Ciesielski and M. Wałęsa, *Polyhedron*, 2006, **25**, 2643.
40 V. Patroniak, A. R. Stefankiewicz, J.-M. Lehn and M. Kubicki, *Eur. J. Inorg. Chem.*, 2005, 4168.
41 F. R. Heirtzler, M. Neuburger, M. Zehnder and E. C. Constable, *Liebigs Ann.*, 1997, 297.
42 V. Patroniak, M. Kubicki, A. R. Stefankiewicz and A. M. Grochowska, *Tetrahedron*, 2005, **61**, 5475.
43 M. Wałęsa-Chorab, A. R. Stefankiewicz, A. Gorczyński, M. Kubicki, J. Kłak, M. J. Korabik and V. Patroniak, *Polyhedron*, 2011, **30**, 233.
44 F. H. Allen, *Acta Crystallogr., Sect. B: Struct. Sci.*, 2002, **58**, 380.
45 S.P. Argent, H. Adams, T. Riis-Johannessen, J. C. Jeffery, L. P. Harding, O. Mamula and M. D. Ward, *Inorg. Chem.*, 2006, **45**, 3905.
46 O. Kahn, *Molecular Magnetism*, Willey-VCH, Weinheim, 1993, 114.
47 J. Curély, *Europhys. Lett.*, 1995, **32**, 529.
48 J. Curély, *Physica B*, 1998, **245**, 263.
49 J. Curély, *Physica B*, 1998, **254**, 277.
50 J. Curély and J. Rouch, *Physica B*, 1998, **254**, 298.
51 L.-F. Ma, M.-L. Han, J.-H. Qin, L.-Y. Wang and M. Du, *Inorg. Chem.*, 2012, **51**, 9431.
52 G. Beobide, O. Castillo, J. Cepeda, A. Luque, S. Pérez-Yáñez, P. Román and D. Vallejo-Sánchez, *Eur. J. Inorg. Chem.*, 2011, 68 and references therein.

53 M. Wałęsa-Chorab, A. Gorczyński, M. Kubicki, M. J. Korabik and V. Patroniak, *Polyhedron*, 2013, **54**, 260.
54 M. Wałęsa-Chorab, A. R. Stefankiewicz, D. Ciesielski, Z. Hnatejko, M. Kubicki, J. Kłak, M. Korabik and V. Patroniak, *Polyhedron*, 2011, **30**, 730.
55 M. Graf, H. Stoeckli-Evans, A. Escuer and R. Vicente, *Inorg. Chim. Acta*, 1997, **257**, 89.
56 J. Carranza, J. Sletten, C. Brennan, F. Lloret, J. Cano and M. Julve, *Dalton Trans.*, 2004, 3997.
57 H. Grove, J. Sletten, M. Julve and F. Lloret, *J. Chem. Soc., Dalton Trans.*, 2000, 515.
58 G. Beobide, O. Castillo, U. García-Couceiro, J. P. García-Terán, A. Luque, M. Martínez-Ripoll and P. Román, *Eur. J. Inorg. Chem.*, 2005, 2586.
59 G. Beobide, O. Castillo, A. Luque, U. García-Couceiro, J. P. García-Terán and P. Román, *Inorg. Chem.*, 2006, **45**, 5367.
60 T. Ishida, T. Kawakami, S. Mitsubori, T. Nagami, K. Yamaguchi and H. Iwamura, *J. Chem. Soc., Dalton Trans.*, 2002, 3177.
61 F. Lloret, M. Julve, J. Cano and G. De Muno, *Mol. Cryst. Liq. Cryst.*, 1999, **334**, 569.
62 M. S. Caceci, Estimating Error Limits in Parametric Curve Fitting, *Anal. Chem.*, 1989, **61**, 2324.
63 *Agilent Technologies, CrysAlis PRO (Version 1.171.33.36d)*, Agilent Technologies Ltd, 2011.
64 G. M. Sheldrick, *Acta Crystallogr., Sect. B: Struct. Sci.*, 2008, **64**, 112.
65 A. Altomare, G. Cascarano, C. Giacovazzo and A. Gualardi, *J. Appl. Crystallogr.*, 1993, **26**, 343.
66 M. Menelaou, T. Weyhermüller, M. Soler and N. Aliaga-Alcalde, *Polyhedron*, 2013, **52**, 398.
67 Q.-X. Yao, L. Pan, X.-H. Jin, J. Li, Z.-F. Ju and J. Zhang, *Chem.–Eur. J.*, 2009, **15**, 11890.